Design of an Ag Plasmonic Nanowire Waveguide with Long Propagation Distance

Yuan-Fong Chau
Department of Electronic Engineering, Chien Hsin University of Science and Technology, No. 229, Jianxing Rd., Zhongli City, Taoyuan County 32097, Taiwan (R.O.C.)
Email: yfc01@uch.edu.tw

***Abstract*—By coupling light to the charges at nanometal interfaces, surface plasmon (SP) enables researches to control photons in a way they have never done before: at the subwavelength level. Coupling of incident light through an air region into an Ag plasmonic nanowire waveguide (APNW) is a highly difficult challenge of light guiding on the surface of metal nanowire. Surface plasmon polaritons, the electromagnetic waves propagating on the interface between metal and dielectrics, have allowed the modal confinement below the diffraction limit. In this paper, we numerically analyze the coupling effect of an APNW which is covered by a dielectric medium using a finite element method. The coupling effect can be modulated by adjusting the Ag nanowire diameter, the covering dielectric medium width and the wavelength of incident light, the propagation length of SP coupling can be maximized. Simulation results reveal that the field confinement can be significantly improved and the majority of the electric field can be carried on the surface of an APNW. The effects of electric field transport along an APNW due to SP coupling which is investigated for different dimensions and lengths. Accordingly, long propagation lengths of about 41500 nm at an incident wavelength of 715 nm and longer propagation length can be achieved if the more sections of APNW are used. Simulation results offer an efficient method for optimizing SP coupling into an APNW and promote the realization of highly integrated plasmonic devices.**

***Index Terms*—plasmonic nanowire waveguide, finite element method, surface plasmon, long propagation lengths**

I. Introduction

Recently, the need for smaller and faster optical devices has established nanophotonics branch, which has been extensively investigated along with the study of plasmonics. Many experimental and theoretical literatures have demonstrated that, for the dielectric-based photonics, large portion of electromagnetic waves spread over the space and cannot be confined in a small region due to the diffraction limit of light. This limits its ability of reducing optical modal volume to cubic half wavelength scale. Optics of surface plasmon polaritons (SPPs) and, in particular, of plasmonic nanostructures, currently attracts considerable interest. Plasmonics is one of the most promising avenues for device miniaturization that guarantees many merits. The emerging field of plasmonics promises the generation, processing, transmission, sensing and detection of signals at optical frequencies along metallic surfaces much smaller than the wavelengths they carry. Plasmonic technology has applications in a wide range of fields, including biophotonics, sensing, chemistry and medicine [1]-[10]. But perhaps the area where it will have the most profound impact is in optical communications, since plasmonic waves oscillate at optical frequencies and thus can carry information at optical bandwidths. Surface plasmons (SPs) are electromagnetic waves that propagate along the surface of the metal nanoparticles (MNPs) [1]. Nanophotonic wire waveguides play an important role for the realization of highly dense integrated photonic circuits and are deployed for various applications in the design of optoelectronic devices such as optical switches, wavelength filters, low power consumption, efficient device integration, ring resonators, power splitters, ultra-fast operational speed, optical logic gates, optical communication system, and optical-interconnects in network [1]-[17]. These nanoparticle-structured waveguides hold the unique promise for the light guiding at the nanoscale.

The miniaturization of optoelectronic devices and realization of ultra-small integrated circuits strongly demand compact waveguide branches. Among the different kinds of plasmonic waveguides, silver (Ag) nanowires have some unique properties that make them particularly attractive, such as low propagating loss due to their smooth surface and scattering of SPs to photons only at their sharp ends. Since the momentums of the photons and SPs are different, it is a challenge to couple light into SP waveguides efficiently. The confinement light in conventional dielectric waveguide is always limited by the diffraction limited and guidance around sharp bends [18], [19]. SP waveguide can provide far stronger, non-diffraction limited confinement and increase the coupling effect of guiding light around the sharp bend, leading to ultra-small and compact photonic devices and the development of non-optical circuits owing to their subwavelength behavior.

In plasmonics, the important signal processing procedure is performed on SPPs instead of photons. SPPs are electromagnetic waves coupled to charge density oscillations at the interface between a material of negative permittivity and one of positive permittivity (e.g.,

Manuscript received May 25, 2014; revised August 28, 2014.

doi: 10.12720/ijsps.3.1.53-59

a metal and a dielectric medium, respectively). However, when it comes to SPs-based devices, we should pay critical attention to the metallic loss come from metal. It is unavoidable for plasmonic devices to experience high loss due to the high conductance of metals, which creates problems over a wide range of applications based on the plasmonic effect.

In this paper, we numerically analyze an Ag plasmonic nanowire waveguide (APNW) for the propagation of SPs on an Ag nanowire by means of finite element method (FEM) with three-dimensional (3-D) calculations, and develop important design guidelines that are critical for the realization of high-performance optical interconnects through an air region coupled into an APNW. The proposed APNW consists of a metal wire covered with low-index dielectric layers, which is an improved structure of a bare metal wire waveguide with the hybrid mode [20]. It has the merits of ultra-long propagation distance and subwavelength modal confinement simultaneously. The enclosure of a covered dielectric medium and an APNW form open SP models and the electromagnetic fields is effectively confined on the surface of an Ag nanowire to generate high local field enhancement. We compared their optical responses with the different cases of their counterparts in near-field zone. The influences of various incident wavelengths in the range of 300-1600 nm are discussed in our simulations. These results are crucial in designing localized surface plasmon resonance (SPR) sensors and other optical devices based on MNPs and may provide valuable references for waveguiding dielectric-supported metal nanowires for practical applications. The design, analysis, optimization, and physical insights behind them are elaborated in detail.

II. Simulation Method and Models

The problem of electromagnetic analysis on a macroscopic level is the problem of solving Maxwell's equations subject to certain boundary conditions. The SP's propagation constant can be retrieved by solving Maxwell's equation at the interface of a MNP and a dielectric medium, which yields bonded modes for a transverse magnetic (TM) polarization.

The governing equation can be written in the form

$$\nabla \times (\mu_r^{-1} \nabla \times E) - k_0^2 \varepsilon_{rc} E = 0 \quad (1)$$

where ε_{rc} is the complex relative permittivity, E is the electric field intensity, k_0 is the wave vector in free space and μ_r is the complex relative permiability.

For the time-harmonic and eigenfrequency problems, the wave number of free space k_0 is defined as

$$k_0 = \omega(\varepsilon_0 \mu_0)^{1/2} = \frac{\omega}{c} \quad (2)$$

where c is the speed of light in vacuum and ω is the angular frequency. When solving the equations as an eigenfrequency problem the eigenvalue is the complex eigenfrequency $\lambda = -j\omega + \delta$, where δ is the damping of the solution. Using the relation $\varepsilon_r = n^2$, where n is the refractive index, the equation (1) can alternatively be written

$$\nabla \times (\nabla \times E) - k_0^2 n^2 E = 0 \quad (3)$$

When the equation is written using the refractive index, the assumption is that μ_r=1 and σ=0 and only the constitutive relations for linear materials are available. When solving for the scattered field the same equations are used but $E = E_{sc} + E_i$ and E_{sc} is the dependent variable. In optics and photonics applications, the refractive index is often used instead of the permittivity (ε). In materials where μ_r is 1, the relation between the complex refractive index, $n' = n - j\kappa$, and the complex relative permittivity is $\varepsilon_{rc} = n^2$, that is $\varepsilon'_r = n^2 - \kappa^2$, $\varepsilon''_r = 2n\kappa$. The inverse relations are

$$n^2 = \frac{1}{2}[\varepsilon'^2_r + (\varepsilon'^2_r + \varepsilon''^2_r)^{\frac{1}{2}}] \quad (4)$$

$$k^2 = \frac{1}{2}[-\varepsilon'_r + (\varepsilon'^2_r + \varepsilon''^2_r)^{\frac{1}{2}}] \quad (5)$$

The parameter κ represents a damping of the electromagnetic wave.

The dispersion properties of the MNP must be considered here since the absorption and permittivity of the metallic material are frequency dependent. The Drude-Lorentz dispersion model is used to describe the dependence of the metallic permittivity on the frequency [21], which can be written as

$$\varepsilon_0 = \varepsilon_\infty + \sum_{j=1}^{M} (f_j \omega_p^2) / (\omega_{0j}^2 - \omega^2 + i\Gamma_j \omega) \quad (6)$$

where ε_∞ is the high-frequency contribution to the relative permittivity, ω_P is the plasma frequency, f_j is the oscillator strength, ω_{0j} is the resonance frequency, and Γ_j is the damping coefficient.

Throughout this paper, we consider an Ag nonowire, illuminated by a plane wave with the TM plane wave. For the Ag permittivity $\varepsilon(\lambda)$ as a function of wavelength (λ) we use the bulk data of Johnson and Christy [22] and corrected with the Drude model, which includes the size effect [23]. Note that particles down to 20nm can well be modeled using bulk permittivity. We investigate waveguiding properties of the nanowire-dielectric system using a 3-D FEM [24]-[30]. The computational domain is discretized into a tetragonal mesh with an element size of one tenth of the nanowire diameter (e.g., 10nm for a 100nm diameter nanowire), terminated by perfectly matched layer (PML) boundaries.

The simulation model in this work is an APNW as shown in Fig. 1, which can be characterized by four geometrical parameters, i.e., d_1, d_2, d_3, d_4, respectively. The structure under study is an Ag nanwire with diameter d_1 and length d_4 surrounded by a dielectric medium, SiO_2, as shown in Fig. 1. The Ag nanowire diameter is much shorter than the wavelength, while the length can be longer than the wavelength. Fig. 1 shows an APNW with Ag nanowire diameter of d_1, length of d_4. The APNW is covered by SiO_2 with a width of d_2. All fixing values of geometrical parameters are given in the inset of Fig. 1. In this case, the APNW is illuminated by a TM plane incident wave which width is set to be 350nm. The incident plane wave is launched away a distance of d_3=350nm from the input end through an air region into

an APNW. The amplitude of incident electric field is set to be 1V/m. Fig. 2 also shows the schematic mesh of simulation model consisting of 20150 elements.

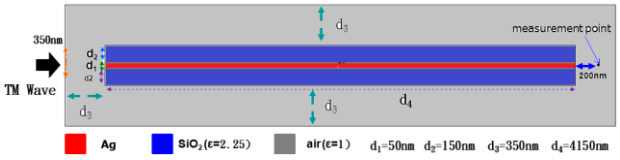

Figure 1. Schematic plot of Ag plasmonic nanowire waveguide (APNW).

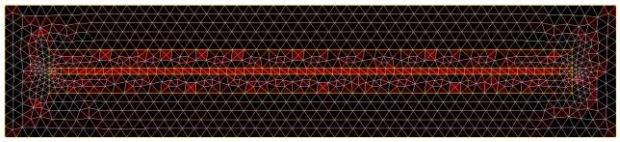

Figure 2. Schematic mesh of simulation model consisting of 20150 elements.

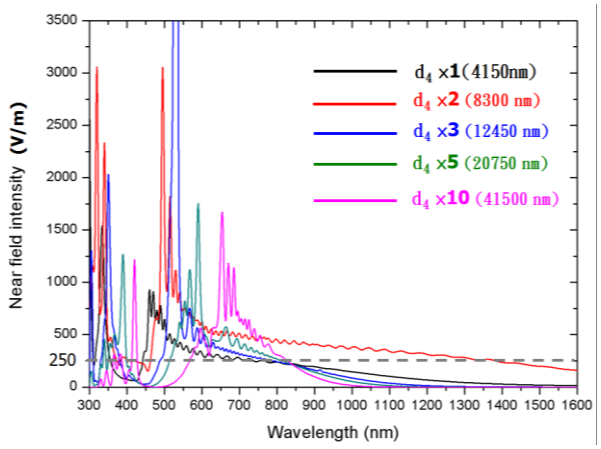

Figure 3 Near-Field intensities as a function of wavelengths for the cases of different length of an APNW (d_4=4150, 8300, 12450, 20750 and 41500nm, respectively) measured at a distance of 200 nm away from the distal end of an APNW.

III. Design, Results and Discussion

Near-field intensities as a function of wavelengths for the cases of different length of an APNW (d_4=4150, 8300, 12450, 20750 and 41500nm, respectively) measured at a distance of 200nm away from the distal end of an APNW is shown in Fig. 3. It can be observed from Fig. 3 that the near-field intensities can be modulated by the length of an APNW (d_4) and the SPR peak wavelengths corresponding to various d_4. It is shown that the near-field intensities measured at measurement point for all cases can achieve a magnitude over 250V/m [see the dashed gray line in Fig. 3] as the incident wavelength raging in λ=560-850nm (showing a broad band propagation). The apparent SPR peak wavelengths raging in λ=450-800nm occur at λ=475nm for the case of d_4=4150nm, λ=510nm for the case of d_4=8300nm, λ=525nm for the case of d_4=12450nm, λ=600nm for the case of d_4=20750nm, and λ=660nm for the case of d_1=41500nm, respectively. Besides, the red-shift trend with the increase of the value of d_4 due to the fact that this red shift depends on the suitable mode itself: the larger the wavelength of the eigenmode, the greater the red-shifted, and the more spread out the SPRs [31], [32]. The analysis of this spectrum shown in Fig. 3 reveals three viewpoints. (1)With increasing the length of an APNW (d_4), the linewidth of the Fabry-Perot resonator modes increases [33]. (2) Electric field intensity minima from the input end of an APNW correspond to maxima from the distal end of an APNW and vice versa, which strongly confirms the explanation of optically excited an APNW as a Fabry-Perot resonator [33]. (3) The modulation field intensities reveal in varies with both wavelength and the length of an APNW (d_4).

Fig. 4(a)-Fig. 4(e) show the corresponding near-field distributions of different length of APNW (d_4) at their selected peak wavelengths, which shows that the electric field distribution on the surface of an APNW can clearly be seen.

An interesting result, namely, some nodal fields, was found on the surface of the APNW. When d_1 is kept constant (d_1=50nm) and d_4 is increased from 4150nm to 41500nm [i.e., d_4×1~d_4×10, see Fig. 3], the nodal field pattern will be changed for various SPR wavelengths of the incident light. In our simulation, the zero-order mode is observed to have no nodal field oscillation along the APNW. This mode has a finite charge and can be regarded as oscillations with an infinite wavelength—thus it cannot be excited by an external electromagnetic wave. The lowest mode with physical meaning is a dipolar mode with one nodal field around the APNW, which has positive and negative charge accumulated at opposite ends of the APNW. This mode can be excited by a field polarized along the *x*-axis and respond at a longer wavelength. Another mode can be identified by the number of nodal fields on the surface of the APNW. It is worthwhile to note that here only even numbers of nodal fields can be found on the surface of the APNW in our simulation. This result is very different from that obtained by means of the boundary element method [34], which includes odd and even modes simultaneously. The discrepancy between our FEM simulation model and the boundary element method in [35] can be attributed to the fact that the *x* polarization incident field always piles up the positive and negative charge pairs along the propagation direction of the APNW, and no net dipole exists in the charge distribution obtained in our simulation. Thus, only an even number of nodal fields can be found on the surface of the APNW. For even-order modes, the wavelengths decrease as additional longitudinal nodes (positive and negative charge pairs) are added. It can be seen in Fig. 4(a)-Fig. 4(e) for the case with d_1=50nm that the number of nodal fields around the APNW for the longitudinal mode is dependent on the aspect ratio (d_4/d_1), which corresponds to different eigenmodes and frequencies (wavelengths). As the aspect ratio (d_4/d_1) increases, the nodal field number increases as d_4 increases. On the basis of our simulations (results are not shown here), a longer spot size of nodal field around the APNW can be produced as d_1 decreases.

In these examples, SPPs propagate along Ag-SiO_2 interfaces. The SiO_2-layer thicknesses can vary from nanometers (smaller than the optical wavelength) to a few hundred nanometers. The plots in Fig. 4(a)~Fig.4(d) indicate the strength of the electric field with increasing

distance to the APNW. This result verified that the incident plane wave can be used to excite SPs in a metallic nanowire and coupled optical information through a free space into a nanoscale optical device. The SP can only be excited at one wire end due to the crystalline nature of the wire. This APNW structure has fair propagation distance when APNW is surrounded by the dielectric material.

One can also see that the electric field is along the radial direction and this mode can be interpreted as a mode formed by rolling-up the mode on the surface of the APNW. This extremely small optical mode area may enable efficient device miniaturization. On the other hand, the confined mode on the surface of the APNW shows extremely low-loss characteristics, micro-scale propagation distances, with the subwavelength modal confinement. A further reduction of the propagation loss is achievable as the radius of the Ag nanowire is decreased while still maintaining the subwavelength modal confinement.

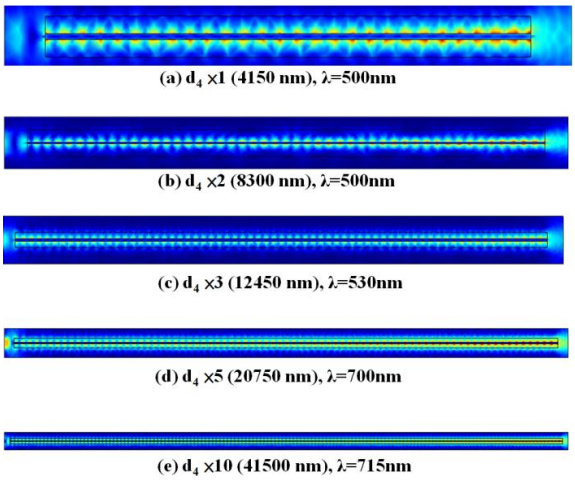

Figure 4. Corresponding near-field distributions of different length (d4) of APNW at their selected peak wavelengths.

Since SPs on the Ag-SiO_2 interface are TM incident light waves, there will be only one component of the magnetic field (H_y). Thus the light wave equations for magnetic fields in the two media, i.e., Ag and SiO_2, are considered for determining the plasmon dispersion relationship:

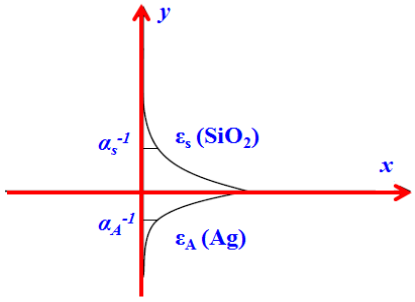

Figure 5. Corresponding schematic representation of a surface plasmon.

The guiding interface coincides with the (x, z) plane, and the wave propagates along the x-axis. α_S^{-1} and α_A^{-1} are the penetration depths of the light wave into the SiO_2 and Ag, respectively.

$$\frac{\partial^2 H_{S,A}}{\partial x^2} + \frac{\partial^2 H_{S,A}}{\partial y^2} + \frac{\omega^2}{c^2}\varepsilon_{S,A} = 0 \quad (7)$$

where H is the y-component of the magnetic field, c is for the speed of light and ω is for the angular frequency. The solutions of the wave equation in (7) are sought in the form of a SP wave propagating along the x-axis and exponentially decaying in both the SiO_2 and Ag (see Fig. 5):

$$H_S = H_0 e^{ikx - i\omega t - \alpha_S y} \quad (8)$$

$$H_A = H_0 e^{ikx - i\omega t - \alpha_A y} \quad (9)$$

where k is the wave number and t is the time. The equations for the reciprocal penetration depths are obtained by substituting the solutions (8) and (9) into the wave equation (7):

$$\alpha_S = (k^2 - \frac{\omega^2}{c^2}\varepsilon_S)^{\frac{1}{2}} \quad (10)$$

$$\alpha_A = (k^2 - \frac{\omega^2}{c^2}\varepsilon_A)^{\frac{1}{2}} \quad (11)$$

The dispersion relationship for a SP is decided by the conventional boundary conditions at the Ag-SiO_2 interface that should be satisfied by the solutions (7) and (11). Using these conditions, we obtained the wave number for SPs as [36]-[40]:

$$k = \frac{\omega}{c}(\frac{\varepsilon_S \varepsilon_A}{\varepsilon_S + \varepsilon_A})^{\frac{1}{2}} \quad (12)$$

From this equation, it can be seen that if εA is negative and larger in magnitude than that of εs, then k is positive, real, and larger than ks=(ω/c)$\varepsilon^{1/2}$ - the wave number of bulk wave in medium SiO_2. Therefore, SPPs are indeed surface waves, i.e., propagating along the surface and exponentially decaying into the surrounding media [41], [42].

In the proposed APNW, it has been found that there are two types of guided mode: one is a strongly confined mode which shows symmetry mode (the first mode, see Fig. 6(a)) and the other is a mode of dipole-like shaped profile, i.e., anti-symmetry mode, which shows an ultra-long propagation distance (the second mode, see Fig. 6(b)). The characteristics of those modes are discussed in the following text.

If the covered dielectric medium (SiO_2) is the same on the both ends of the APNW, the SPs couple to form two modes: symmetric [see Fig. 6(a)] and anti-symmetric (see Fig. 6(b)] [43]-[45]. One of the predominant differences between the two modes is the distribution of the electric field. A symmetric Ag nanowire SP has a symmetric distribution of the electric field [e.g., see Fig. 6(c)]. However, an anti-symmetric Ag nanowire SP is characterized by an anti-symmetric distribution of the electric field [e.g., see Fig. 6(d)]. As the diameter of Ag nanowire is increased [e.g., d_1=200nm as shown in Fig. 6(c)], the wave number of the symmetric mode tends towards a bulk wave in the surrounding SiO_2 [46], [47]. The wave number of the anti-symmetry mode is increased as the diameter of Ag nanowire is decreased [e.g., d_1=50nm as shown in Fig. 6(d)]. This phenomenon

can be interpreted by considering the charge distribution across the Ag nanowire covered by the dielectric medium (SiO_2) for the symmetric [see Fig. 6(a) and Fig. 6(c)] and anti-symmetric modes [see Fig. 6(b) and Fig. 6(d)]. It can be seen in Fig. 6(a) and Fig. 6(b) that the symmetric mode for anti-symmetric charge distribution and the anti-symmetric mode for symmetric charge distribution. Thus the electric field will also have an anti-symmetric distribution across the Ag nanowire for a symmetric charge and a symmetric distribution across the Ag nanowire for an anti-symmetric charge. The dispersion relations for the symmetric and anti-symmetric SPs for an Ag nanowire (diameter d_1) of permitivity ε_A surrounded by SiO_2 (width d_2) with permitivity ε_s may be derived by using Maxwell's equations, conventional boundary conditions and seeking a solution in the form of SPs propagation on the Ag-SiO_2 interfaces. The symmetric and anti-symmetric dispersion relations are given respectively by [48]

$$\frac{\varepsilon_S}{\varepsilon_A} = \frac{-k_{2z}}{k_{1z}}\left[coth\left(\frac{d_1}{2i}\right)k_{2z}\right] \quad (13)$$

$$\frac{\varepsilon_S}{\varepsilon_A} = \frac{k_{2z}}{k_{1z}}\left[tanh\left(\frac{d_1}{2i}\right)k_{2z}\right] \quad (14)$$

where ε_A is the dielectric function of the Ag nanowire surround on both sides by ε_S, k_{2z} and k_{1z} are the perpendicular components of the wavevector inside and outside the Ag nanowire respectively, and d_1 is the diameter of the Ag nanowire. It should be noted that these expression are for the symmetric situation where the medium on both side of the Ag nanowire are the same.

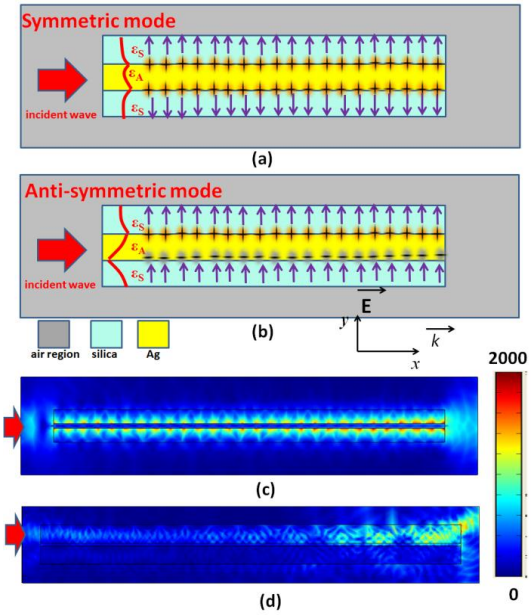

Figure 6. (a) Symmetric mode (the direction of the normal components of electric field for a structure with symmetric surface charges): the direction of the electric field for an APNW with symmetric surface charges and (b) Anti-symmetric mode (the direction of the normal components of electric field for a structure with anti-symmetric surface charges): the direction of the electric field for an APNW with anti-symmetric surface charges. (c) A selected symmetric mode for the case of an APNW, d1=50nm, d2=150nm, d3=350nm, d4=4150nm, at a light wavelength of 500nm. (d) A selected anti-symmetric mode for the case of an APNW, d1=50nm, d2=150nm, d3=350nm, d4=4150nm, at a light wavelength of 1500nm.

IV. Conclusions

In conclusion, it is a highly difficult challenge of light guiding through an air region into an SP waveguide. In this paper, we have numerically analyzed an APNW and developed the key design guidelines that ensure effective propagation of incident light through an air region into an APNW. The proposed structure of APNW is an important novel geometry for plasmonic MNPs, combining the highly attractive nanoscale optical properties of both a metallic nanowire and the covering dielectric medium. Numerical investigation by using a 3-D FEM indicates that the confinement of SPs fields of an APNW can be significantly improved if the metallic nanowire is covered with a dielectric medium. Accordingly, large propagation lengths of about 41500nm at a light wavelength of 715nm and longer propagation length if the more sections of APNW are used. Our results will be useful for the optimum design of metallic nanowires as interconnects for high-density nanophotonic circuit integration and promotes the realization of highly integrated plasmonic devices, such as plasmonic mode-gap waveguides [49], cross-index-modulation plasmonic waveguides [50], hybrid plasmonic waveguide [51], and so on [52]-[56]. This allows low power operation and integration on a chip in a variety of applications such as nanolasers [52], modulators [53], splitters [54] and metal-dielectric-metal waveguide [55], metal patch waveguide [56].

Acknowledgment

The authors are thankful for the financial support from National Science Council, Taiwan, ROC, under Grant number NSC 102-2112-M-231-001-.

References

[1] G. Veronis and S. Fan, "Bends and splitters in metal-dielectric-metal subwavelength plasmonic waveguides," *Appl. Phys. Lett.*, vol. 87, no. 13, pp. 131102, 2005.

[2] X. Guo, *et al.*, "Direct coupling of plasmonic and photonic nanowires for hybrid nanophotonic components and circuits," *Nano Lett.*, vol. 9, no. 12, pp. 4515-4519, 2009.

[3] P. Bharadwaj, B. Deutsch, and L. Novotny, "Optical antennas," *Adv. Opt. Photon.*, vol. 1, no. 3, pp. 438-483, 2009.

[4] E. Verhagen, M. Spasenović, A. Polman, and L. Kuipers, "Nanowire plasmon excitation by adiabatic mode transformation," *Phys. Rev. Lett.*, vol. 102, no. 20, pp. 203904, 2009.

[5] D. Anuj, C. Michael, and V. D. Tuan, "Bimodal behavior and isobestic transition pathway in surface plasmon resonance sensing," *Optics Express*, vol. 20, no. 21, pp. 23630-23642, 2012.

[6] Y. F. Chau, M. W. Chen, and D. P. Tsai, "Three-Dimensional analysis of surface plasmon resonance modes on a gold nanorod," *Applied Optic*, vol. 48, no. 3, pp. 617-622, 2009.

[7] S. A. Maier, *Plasmonics: Fundamentals and Applications*, New York: Springer, 2007.

[8] W. L. Barnes, A. Dereux, and T. W. Ebbesen, "Surface plasmon subwavelength optics," *Nature*, vol. 424, no. 6950, pp. 824-830, 2003.

[9] M. Khajavikhan, *et al.*, "Thresholdless nanoscale coaxial lasers," *Nature*, vol. 482, no. 7384, pp. 204-207, 2012.

[10] M. Nomura, N. Kumagai, S. Iwamoto, Y. Ota, and Y. Arakawa, "Laser oscillation in a strongly coupled singlequantum-dot-nanocavity system," *Nat. Phys.*, vol. 6, no. 4, pp. 279-283, 2010.

[11] K. F. MacDonald, Z. L. Sámson, M. I. Stockman, and N. I. Zheludev, "Ultrafast active plasmonics," *Nat. Photonics*, vol. 3, no. 1, pp. 55-58, 2009.

[12] A. Y. Elezzabi, Z. Han, S. Sederberg, and V. Van, "Ultrafast all-optical modulation in silicon-based nanoplasmonic devices," *Opt. Express*, vol. 17, no. 13, pp. 11045-11056, 2009.

[13] M. I. Stockman, "The spaser as a nanoscale quantum generator and ultrafast amplifier," *J. Opt.*, vol. 12, no. 2, pp. 024004, 2010.

[14] J. A. Dionne, L. A. Sweatlock, H. A. Atwater, and A. Polman, "Plasmon slot waveguides: Towards chip-scale propagation with subwavelength-scale localization," *Phys. Rev. B*, vol. 73, no. 3, pp. 035407, 2006.

[15] L. Y. M. Tobing, L. Tjahjana, and D. H. Zhang, "Demonstration of low-loss on-chip integrated plasmonic waveguide based on simple fabrication steps on silicon-on-insulator platform," *Appl. Phys. Lett.*, vol. 101, no. 4, pp. 041117, 2012.

[16] J. H. Kang, Y. S. No, S. H. Kwon, and H. G. Park, "Ultrasmall subwavelength nanorod plasmonic cavity," *Opt. Lett.*, vol. 36, no. 11, pp. 2011-2013, 2011.

[17] J. A. Dionne, K. Diest, L. A. Sweatlock, and H. A. Atwater, "PlasMOStor: A metal-oxide-Si field effect plasmonic modulator," *Nano Lett.*, vol. 9, no. 2, pp. 897-902, 2009.

[18] L. Tong, J. Lou, and E. Mazur, "Single-Mode guiding properties of subwavelength-diameter SiO_2 and silicon wire waveguides," *Optics Express*, vol. 12, pp. 1025-1035, 2004.

[19] M. Law, *et al.*, "Nanoribbon waveguides for subwavelength photonics integration," *Science*, vol. 305, pp. 1269-1273, 2004.

[20] R. F. Oulton, V. J. Sorger, D. A. Genov, D. F. P. Pile, and X. Zhang, "A hybrid plasmonic waveguide for subwavelength confinement and long-range propagation," *Nat. Photonics*, vol. 2, no. 8, pp. 496-500, 2008.

[21] C. F. Bohren and D. R. Huffman, *Absorption and Scattering of Light by Small Particles*, Wiley, 1983.

[22] D. F. P. Pile and D. K, Gramotnev, "Plasmonic subwavelength waveguides: Next to zero losses at sharp bends," *Opt. Lett.* vol. 30, pp. 1186-1188, 2005.

[23] M. Young, *The Technical Writer's Handbook*. Mill Valley, CA: University Science, 1989.

[24] J. Jin, *The Finite Element Method in Electromagnetics*, New York: John Wiley and Sons, Inc., 2002.

[25] M. Ameen, *Computational Elasticity: Theory of Elasticity, Finite and Boundary Element Methods*, New Delhi, India: Narosa Publishing House, 2005.

[26] O. Axelsson, *Finite Element Solution of Boundary Value Problems: Theory and Computation*, Philadelphia, Philadelphia: Society for Industrial and Applied Mathematics, 2001.

[27] K. J. Bathe, *Finite Element Procedures*, New Delhi, India: PHI Learning, 2009.

[28] C. R. Alavala, *Finite Element Method: Basic Concepts and Applications*, New Delhi, India: PHI Learning, 2009.

[29] Z. Chen, *The Finite Element Method: Its Fundamentals and Applications in Engineering*, 2nd ed. New Jersey, USA: World Scientific, 2011.

[30] R. Cook, *Concepts and Applications of Finite Element Analysis*, New Delhi, India: Wiley, 2002.

[31] D. R. Mason, D. K. Gramotnev, and K. S. Kim, "Wavelength-Dependent transmission through sharp 90◦ bends in sub-wavelength metallic slot waveguides," *Opt. Express*, vol. 18, pp. 16139-16145, 2010.

[32] Y. J. Chang and Y. C. Liu, "Polarization-Insensitive subwavelength sharp bends in asymmetric metal/multi-insulator configuration," *Optics Express*, vol. 19**,** pp. 3063-3076, 2011.

[33] D. K. Gramotnev and K. C. Vernon, "Adiabatic nano-focusing of plasmons by sharp metallic wedges," *Appl. Phys. B.*, vol. 86, pp. 7-17, 2007.

[34] J. Aizpurua, *et al.*, "Optical properties of coupled nanoscale metallic rods for field-enhanced spectroscopy," *Phys. Rev. B*, vol. 71, pp. 235420, 2005.

[35] T. Okamoto, "Near-Field spectral analysis of metallic beads," in *Near-Field Optics and Surface Plasmon Polaritons*, S. Kawata, Ed. Springer, 2001, pp. 99.

[36] Y.-F. Chau, *et al*., "Modeling and simulation of a high sensitivity biosensor in a periodic array of metal nanorod pair by using the finite element method," *Journal of Advances in Mathematics*, vol. 5, no. 3, pp. 783-791, Jan. 2014.

[37] C.-C. Hu, W. Yang, Y.-T. Tsai, and Y.-F. Chau, "Gap enhancement and transmittance spectra of a periodic bowtie nanoantenna array buried in a SiO_2 substrate," *Optics Communications*, vol. 324, pp. 227-233, Apr. 2014.

[38] C.-C. Hu, Y.-T. Tsai, W. Yang, and Y.-F. Chau, "Effective coupling of incident light through an air region into an s-shape plasmonic Ag nanowire waveguide with relatively long propagation length," *Plasmonics*, vol. 9, pp. 573-579, 2014.

[39] Y.-F. Chau and C.-Y. Jheng, "Buried effects of surface plasmon resonance modes for periodic metal-dielectric nanostructures consisting of coupled spherical metal nanoparticles with cylindrical pore filled with a dielectric," *Plasmonics*, vol. 9, pp. 1-9, 2014.

[40] W. Yang, Y.-F. Chau, and S.-C. Jheng, "Analysis of transmittance properties of surface plasmon modes on periodic solid/outline bowtie nanoantenna arrays," *Phys. Plasmas*, vol. 20, pp. 064503, Jun. 2013.

[41] Y.-F. Chau, W.-H. Lin, C.-Y. Jheng, S.-C. Jheng, M.-J. Sung, and D. P. Tsai, "Numerical investigation of a castle-like contour plasmonic nanoantenna operating wavelengths in ultraviolet-visible, visible light and infrared light," *Plasmonics*, vol. 8, pp. 755-761, 2013.

[42] Y.-F. Chau, "Long-Ranging propagation based on resonant coupling effects using series connection of ten nanoshells in plasmon waveguide," *Applied Optics*, vol. 51, pp. 640-643, May 2012.

[43] T. Nikolajsen, K. Leosson, I. Salakhutdinov, and S. I. Bozhevolnyi, "Polymer-Based surface-plasmon-polariton stripe waveguides at telecommunication wavelengths," *Applied Physics Letters*, vol. 82, pp. 668-670, 2003.

[44] E. N. Economon, "Surface-Plasmonin thin films," *Physical Review*, vol. 182, pp. 539-554, 1969.

[45] D. Sarid, "Long-Range surface-plasma waves on very thin metal films," *Phys. Rev. Lett.*, vol. 47, pp. 1927-1930, 1981.

[46] W. L. Barnes, A. Dereux, and T. W. Ebbesen, "Surface plasmon subwavelength optics," *Nature*, vol. 424, pp. 824-830, 2003.

[47] S. A. Maier, *et al.*, "Local detection of electromagnetic energy transport below the diffraction limit in metal nanoparticle plasmon waveguides," *Nat. Mater.*, vol. 2, pp. 229-232, 2003.

[48] Quail, *et al.*, "Long range surface-plasmon modes in silver and aluminum films," *Optics Letters*, vol. 8, pp. 377-379, 1983.

[49] S. Lee and S. Kim, "Plasmonic mode-gap waveguides using hetero-metal films," *Opt. Express*, vol. 18, no. 3, pp. 2197-2208, 2010.

[50] R. Hao, E. Li, and X. Wei, "Two-Dimensional light confinement in cross-index-modulation plasmonic waveguides," *Opt. Lett.*, vol. 37, no. 14, pp. 2934-2936, 2012.

[51] R. F. Oulton, V. J. Sorger, D. A. Genov, D. F. P. Pile, and X. Zhang, "A hybrid plasmonic waveguide for subwavelength confinement and long-range propagation," *Nat. Photonics*, vol. 2, no. 8, pp. 496-500, 2008.

[52] V. J. Sorger and X. Zhang, "Physics spotlight on plasmon lasers," *Science*, vol. 333, no. 6043, pp. 709-710, 2011.

[53] V. J. Sorger, N. D. L. Kimura, R. M. Ma, and X. Zhang, "Ultra-Compact silicon nanophotonic modulator with broadband response," *Nanophotonics*, vol. 1, no. 1, pp. 17-22, 2012.

[54] L. A. Sweatlock and K. Diest, "Vanadium dioxide based plasmonic modulators," *Opt. Express*, vol. 20, no. 8, pp. 8700-8709, 2012.

[55] F. Lou, D. Dai, and L. Wosinski, "Ultracompact polarization beam splitter based on a dielectric-hybrid plasmonic-dielectric coupler," *Opt. Lett.*, vol. 7, no. 16, pp. 3372-3374, 2012.

[56] K. Leosson, T. Nikolajsen, A. Boltasseva, and S. I. Bozhevolnyi, "Long-Range surface plasmon polariton nanowire waveguides for device applications," *Opt. Express*, vol. 14, no. 1, pp. 314-319, 2006.

Yuan-Fong Chau was born in Hualian, Taiwan on Aug. 23, 1963. He received his M.S. of Electronic Engineering in Chung Chein Institude of Techonology, Da-Shi, Taiwan from 1983-1985. He also received his M.S. of Physics in National Taiwan University from 1999-2001. He recieved his Ph.D degree in Department of Electrophysics from Chiao Tung University, Taiwan from 2001-2004.

From 1985 to 2004 he was an officer of Taiwan Army. He was an Assistant Professor at department of electrical Engineering, Lee Min institute of technology, New Taipei city, Taiwan from 2004 to 2005. From 2005 to 2008 he was an Assistant Professor in department of electrical engineering, Ching Yun University, Zhongli, Taiwan. From 2008 to 2012 he was an Associate Professor in department of electrical engineering, Ching Yun University, Zhongli, Taiwan. Now he is a Professor in department of electrical engineering, Chien Hsin University of Science and Technology, Zhongli, Taiwan.

He is author and coauthor of 100 journal papers and more than 150 conference papers. He had 15 patents in Taiwan. His current research interests are optic fiber communication, electromagnetic simulation, nano-photonics, near-field optics, plasmonics, meta-materials, bio-photonics and their applications. He was invited as an invited speaker for international conference or symposium more than 10 times. Besides, He have received a number of prestigious awards, such as "Best poster paper awarded, The international conference on nanophotonics 2010, Tsukuba, Japan, 2010", "Best paper award in Communications, The 2014 International Electrical Engineering Congress", Silver Medal, "The international Innovative Invention Poster Competition for Biotechnology, Taiwan, 2010", and "Award for publication of Taiwan aboriginal people, 2008-2013" and some of other awards.